

1 **Response to Referee #1:**

2 **General comment:**

3 *The authors present a study where they determined the number of cloud condensation*
4 *nuclei (CCN) using a new method based on nephelometer measurements. They claim that this*
5 *method is more convenient and cheaper than traditional measurements. Several studies have*
6 *been published over the last 10 years that show that humidified nephelometer measurements*
7 *can be used to infer CCN concentrations. They make several assumptions and use of various*
8 *additional parameters. The apparent difference of the current study is the fact that no*
9 *measurements of the particle number size distribution (PNSD). The manuscript contains*
10 *several obscure sections and mistakes (grammar, typos). In addition, the method is poorly*
11 *described and compared to previous work. Several sections are not well organized. A major*
12 *revision considering my detailed comments below might help to improve the manuscript such*
13 *that it may be considered for publication. In addition, the complete manuscript should be*
14 *carefully proofread.*

15 **Response:** Thanks for your comments. Comments are addressed point-by-point and
16 corresponding responses are listed below. The whole manuscript is also checked.

17

18 **Major comments:**

19 *1) Applicability of the new method*

20 *The caveats of the new method should be made clear in the abstract and conclusions. It is*
21 *mentioned that it cannot be applied for externally mixed aerosol and particle populations with*
22 *many large particles (e.g. dust, sea salt). Are there situations when $\Delta\kappa$ is too*
23 *large/small that this bias will influence $N(\text{CCN})$? Does the shape of the aerosol distribution*
24 *play a role? Would, for example, multiple modes affect the Angstrom coefficient such that it*
25 *exceeds 1.5?*

26 **Response:** Thanks for the suggestion.

27 Hygroscopicity of both inorganic compounds and black carbon remain about the same
28 under different saturated conditions, and the increase of hygroscopicity under supersaturated
29 conditions are generally caused by organic compounds (Wex et al., 2009; Renbaum-Wolff et
30 al., 2016). In ambient atmosphere, particles are consist of diverse compositions and the
31 difference of particle hygroscopicity under different saturated conditions can be expected to
32 be limited within a small range. However, in regions near strong sources of only one specific
33 composition, this specific composition can completely dominate and lead to too large or too
34 small $\Delta\kappa$. As a result, in regions with strong sources of a single composition, $\Delta\kappa$ can be too

35 large or too small and lead to significant deviations of predicted N_{CCN} .

36 Particle number size distribution (PNSD) is important for aerosol activation and aerosol
37 scattering. In this study, both aerosol activation and aerosol scattering are considered to be
38 dominated by particles of accumulation mode and the shape of PNSD is taken in account to
39 some extent by $\Delta\kappa$ ranging from 0.5 to 1.5. When aerosol populations consist of large number
40 of particles of Atiken mode which can contribute significantly to aerosol scattering, $\Delta\kappa$ can
41 exceed 1.5 and N_{CCN} predicted by this new method can be overestimated.

42 We have added corresponding descriptions in the abstract, results and conclusions as
43 follows:

44 Abstract, Line 20: “...is established to predict N_{CCN} . Due to the precondition for the
45 application, this new method is not suitable for externally mixed particles, large particles (e.g.
46 dust and sea salt) or particles near single source regions. ...”

47 Results, the last line of the second-to-last paragraph: “... In regions of single aerosol
48 emissions or productions, the actual $\Delta\kappa$ can be too large (some organic compositions, Wex et
49 al., 2009; Renbaum-Wolff et al., 2016) or too small (inorganic compositions and black carbon)
50 and thus is not suitable for the application of this method.”

51 Conclusions, the last line of second paragraph: “... under conditions without sea salt
52 aerosol, dust aerosol, externally mixed aerosol or aerosol near single source regions.”

53

54 2) Comparison to previous studies

55 I suggest adding a table listing previous studies that have used optical aerosol parameters
56 to infer N_{CCN} . This table should include the parameters that were used (PNSD etc), air
57 mass characteristics (aged or not), caveats of the method and comments on results/findings.
58 This way, the necessity of measurements for various air masses will be more obvious and the
59 applicability of the new method will be clearer. For example, the difference to the methods by
60 Kuang et al. and Brock et al. to the current method is not fully clear.

61 **Response:** Thanks for the suggestion. We have added Table 1 and improved descriptions
62 in the introduction. The methods proposed by Kuang et al. and Brock et al. are used to
63 calculate hygroscopicity parameter and thus is not included in Table 1.

Campaign	Air mass	Parameter	Caveats	Results	Reference
ICARTT ¹ in the north	Polluted air mass	fRH and PNSD	Calculate N_{CCN} with aerosol hygroscopicity	Predict N_{CCN} at SS > 0.3% with a	Ervens et al., 2007

eastern USA and Canada			contrained by f(RH) and PNSD.	0.9 R ² .	
HaChi ² on the North China Plain	Aged continental air mass	PNSD and fRH	Similar to Ervens et al., 2007. Calculate N_{CCN} with the hygroscopicity parameter contrained by f(RH) and PNSD.	Slopes around 1 and R ² around 0.9.	Chen et al., 2014
TARFOX ³ Atlantic seaboard and ACE-2 ⁴	Polluted air mass	Retrieved aerosol volume from remote sensing	Predict N_{CCN} from aerosol volumes with empirical number-to-volume concentration ratio	Overestimate up to 5 times	Gasso and Hegg, 2003
ACE-2 in northeastern Atlantic	Diverse air mass	Backscatter or extinction profile. CCN at the surface.	Retrieve N_{CCN} profile from backscatter (or extinction) vertical profile assuming their ratios are the same to the ratio at surface, which can be calculated by backscatter (or extinction) and N_{CCN} measured at the surface	Predict N_{CCN} on most days for 0.1% SS and on 20%–40% of the days at 1% SS.	Ghan and Collins, 2004
ARM ⁵ Climate Research Facility central site at the Southern Great Plains	Continental air mass	Backscatter (or extinction) and RH profile. fRH and CCN at surface	Same as Ghan and Collins, 2004.	Explains CCN variance for 25%-63% of all measurements at high supersaturations	Ghan et al., 2006
TRACE-P ⁶ and ACE-Asia ⁷	Asian outflow over the western Pacific	Aerosol Index (AI, the product of ambient light extinction and \dot{A})	Predict N_{CCN} based on empirical relationship between AI and N_{CCN}	AI relate well to CCN only with suitably stratified data	Kapustin et al., 2006

Multiple measurements	Diverse air mass	AERONET aerosol optical thickness (AOT)	Predict N_{CCN} based on empirical relationship between AOT and N_{CCN} as a power law	Predict N_{CCN} at $SS > 0.3\%$ with a $0.88 R^2$, but have a factor-of-four range of N_{CCN} at a given AOT	Andreae, 2009
Four ARM sites	Polluted air mass	SSA, backscatter fraction and σ_{sp}	Estimate N_{CCN} from fitting parameters for the N_{CCN} activity spectra, which can be calculated based on their empirical relationships with aerosol optical properties.	Predict N_{CCN} with slopes around 0.9 and R^2 around 0.6.	Jefferson, 2010
Multiple ARM sites around the world	Diverse air mass	RH, fRH, SSA, AOT and σ_{sp}	Calculate N_{CCN} with σ_{sp} (or AOT) based on their empirical relationship, whose impact RH, fRH and SSA.	Achieve the best results by using σ_{sp} and SSA. Weakly affect on the $\sigma_{sp}-N_{CCN}$ relationship by fRH. Deteriorate N_{CCN} -AOT relationship with increasing RH	Liu and Li, 2014
Multiple ARM sites around the world	Diverse air mass not dominated by dust	\dot{A} and extinction coefficient	Calculate N_{CCN} with light extinction based on their empirical relationship.	Deviate typically within a factor of 2.0.	Shinozuka et al., 2015

64 Tabel 1. Review of studies that have used aerosol optical parameters to infer N_{CCN} .

65 ¹ International Consortium for Atmospheric Research on Transport and Transformation.

66 ² Haze in China.

67 ³ Troposphere Aerosol Radiative Forcing Experiment.

68 ⁴ Second Aerosol Characterization Experiment.

69 ⁵ Atmospheric Radiation Measurement.

70 ⁶ Transport and Chemical Evolution over the Pacific.

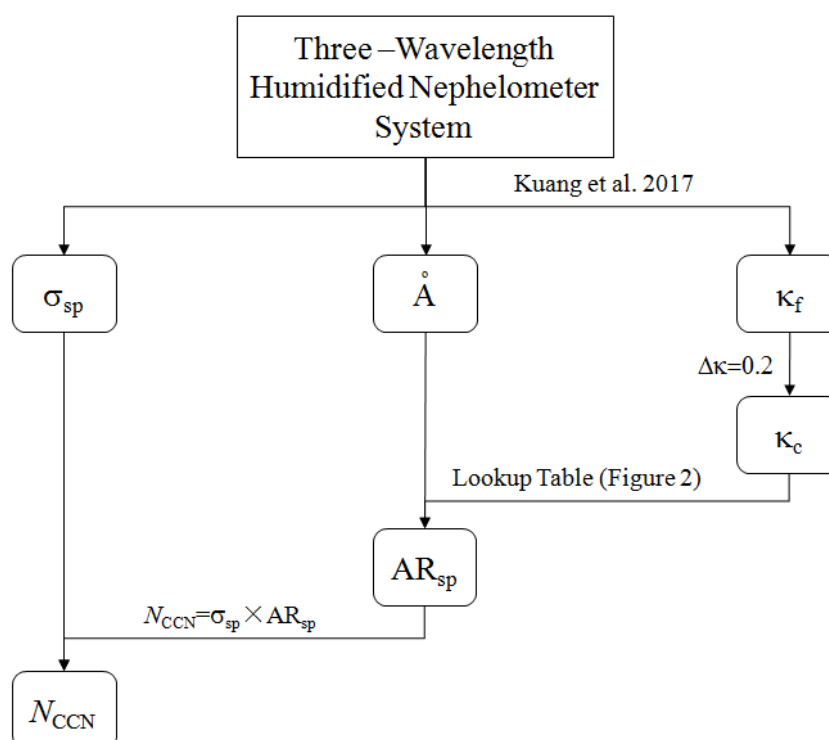
71 ⁷ Aerosol Characterization Experiment–Asia.

72

73 3) *Clarity of method application*

74 a) *While Figure 3 is somewhat helpful, it should be extended to be the central figure of the*
75 *manuscript. Labels can be added to the arrows explaining in detail what is done in each step,*
76 *e.g. a reference to the respective equation would be helpful.*

77 **Response:** Thanks for the suggestion. We have revised Figure 3 as follows:



78

79

80 b) *The comparison to measured $N(\text{CCN})$ is useful and necessary in order to validate the*
81 *new method. However, a few more details about the CCN measurements are needed. At what*
82 *supersaturations were they measured (l. 116)? It is known that CCN measurements are most*
83 *uncertain at low supersaturations. What supersaturation was chosen for the comparison?*

84 **Response:** Thanks for the suggestion. There were five supersaturations (0.07%, 0.10%,
85 0.20%, 0.40% and 0.80%) and N_{CCN} at 0.07% supersaturation was chosen for the comparison,
86 because at higher supersaturations this new method is not applicable any more. We have
87 revised the statement in line 116 as: “Measurements at five supersaturations (0.07%, 0.10%,
88 0.20%, 0.40% and 0.80%) were conducted sequentially with each cycle lasted for 1 hour, and
89 N_{CCN} at 0.07% supersaturation was used in this study.”

90

91 4) *Clarity of language*

92 *At several places, the text is not clear or even wrong and should be revised. Examples*
93 *include:*

94 *l. 57: Aerosol hygroscopicity is defined as the ability of an aerosol particle to take up*
95 *water. Hygroscopicity is not a function of particle size.*

96 **Response:** Thanks for the suggestion. We agree with the reviewer. The statement in the
97 manuscript leads to misunderstanding and we have revised it as: “...aerosol CCN activity is
98 determined by aerosol size and aerosol hygroscopicity. ...”

99

100 *l. 68- 72: It should be clarified which combination of parameters is best suited and which*
101 *problems/deviations (from what?) might occur.*

102 **Response:** Thanks for the suggestion. As mentioned in the response to “2) Comparison to
103 previous studies”, we have revised line 68-72 as follows:

104 *“...due to the diversity of hygroscopicity of less-absorbing components. Thus N_{CCN}*
105 *calculation combining SSA, backscatter fraction and σ_{sp} still lead to significant deviations,*
106 *with a 0.6 R^2 (Jefferson, 2010). As for fRH, there was a study applied aerosol optical*
107 *quantities (σ_{sp} or aerosol optical thickness) with fRH or SSA to calculate N_{CCN} (Liu and Li,*
108 *2014). In their study, compared with the combination of SSA and aerosol optical quantities,*
109 *the combination of fRH and aerosol optical quantities is found to be less effective in*
110 *estimating N_{CCN} , even though fRH directly connected with aerosol hygroscopicity (Liu and Li,*
111 *2014). ...”*

112

113 *l. 143: ‘and can determines ‘kappa’ with A’ is unclear*

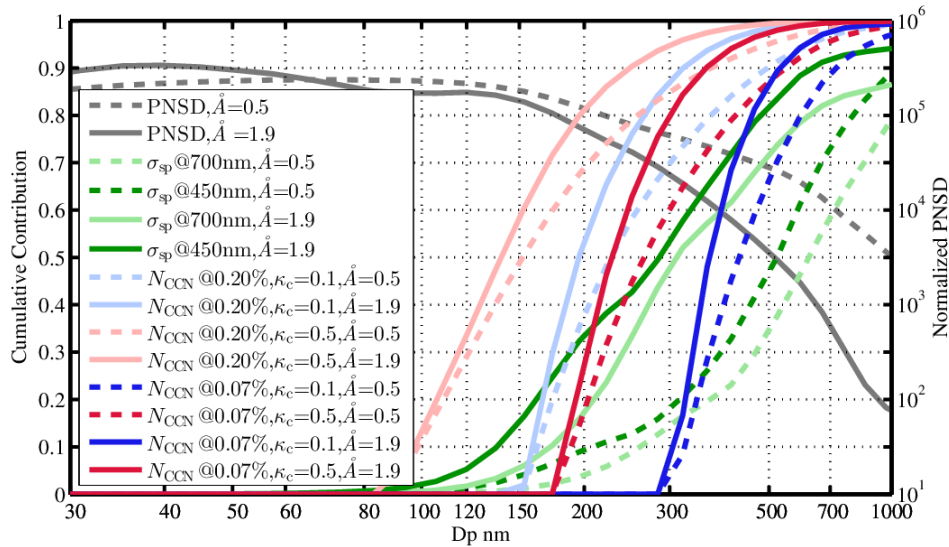
114 **Response:** Thanks for the suggestion. We have revised this sentence as: “... and is found
115 can be used to predict κ_f in combination with \dot{A} in recent studies(Brock et al., 2016;Kuang
116 et al., 2017). This method of calculating κ_f based on κ_{sca} and \dot{A} was confirmed by good
117 agreement with κ_f calculated from fRH and PNSD.”

118

119 *l. 174: This text is hard to follow. At the very least, add numerical ranges for the various*
120 *parameters. It would be even better to connect this discussion to a figure (either an additional*
121 *one or existing one)*

122

Response: Thanks for the suggestion. We have revised Figure 1 as follows:



123

124 Figure 1. Aerosol PNSD (black lines), the cumulative contribution of σ_{sp} at wavelength of
 125 450nm and 700nm (dark green lines and light green lines, respectively), the cumulative
 126 contribution of N_{CCN} at supersaturation of 0.07% (dark red and dark blue lines) and the
 127 cumulative contribution of N_{CCN} at supersaturation of 0.20% (light red and light blue lines)
 128 based on measurement in several campaigns in the North China Plain. Solid lines and dashed
 129 lines indicate \tilde{A} of 1.9 and 0.5, respectively. Blue lines and red lines indicate κ_c of 0.1 and
 130 0.5, respectively.

131 There is a typo error of \tilde{A} value in Figure 1. And we also revised this sentence as
 132 “Because particles smaller than 200nm can activate at supersaturations higher than 0.07%
 133 while scatter less light at wavelengths longer than 450nm, which are shown as the light color
 134 lines in Figure 1, ...”

135

136

137 *l. 198: ‘...which reveals that particles...’ – I do not understand this fragment*

138 **Response:** Thanks for the suggestion. We have revised this sentence as: “This higher
 139 sensitivity of AR_{sp} to \tilde{A} reveals that particles having mean predominate size smaller than
 140 existing particles can contribute more to N_{CCN} . ”

141

142 *l. 214: Do you mean ‘..due to size-dependent hygroscopicity’?*

143 **Response:** Thanks for the suggestion. We have revised it accordingly.

144

145 *l. 284 – 294: This paragraph should be rewritten as I cannot follow the line of thought.*
146 *For example, you start with ‘On one hand, the variation of kappa(c) can be quite large...’ and*
147 *continue later ‘On the other hand, the influence of kappa(c) cannot be ignored . . .’ These two*
148 *sentences should introduce opposing facts, but they do not.*

149 **Response:** Thanks for the suggestion. We have revised this paragraph as follows:

150 *“... First, the variation of κ_c is not always small and can cause non-ignorable deviations*
151 *of calculated N_{CCN} in certain cases. As many studies of N_{CCN} measurement showed, the*
152 *variation of κ_c is often small and a constant κ_c can be used to calculate N_{CCN} accurately*
153 *(Andreae and Rosenfeld, 2008;Gunthe et al., 2009;Rose et al., 2010;Deng et al., 2013).*
154 *Results in this study are similar to these previous studies. However, large variations of κ_c are*
155 *also found in some other studies. In NCP, fluctuations of aerosol hygroscopicity during New*
156 *Particle Formation events and soot emissions lead to significant deviations of calculated*
157 *N_{CCN} from average aerosol hygroscopicity (Ma et al., 2016). Second, the influence of κ_c*
158 *variation on N_{CCN} calculation cannot be ignored because the value of the average*
159 *hygroscopicity differs in various regions during various periods. In summer of NCP, measured*
160 *κ_f at sub-saturated conditions can reach up to 0.45 when inorganic compositions dominate in*
161 *particles (Kuang et al., 2016). ...”*

162

163 *5) Structure*

164 *Essential information should be given as early as possible in the manuscript:*

165 *a) The Angstrom coefficient should be defined in the introduction or in Section 2.*

166 **Response:** Thanks for the suggestion. We have defined Angstrom Exponent in Section 2
167 and we have revised the statement in the introduction in line 47 as: “... Angstrom Exponent
168 (\AA , which is the exponent commonly used to describe the dependence of σ_{sp} on
169 wavelength),...”

170

171 *b) Caveats of the method should be pointed out throughout the paper*

172 **Response:** Thanks for the suggestion. We have added caveats in the abstract and

173 conclusions as presented in lines 50-60 in this reponse.

174

175 *c) It is highly confusing that in Section 2 $\Delta\kappa$ is introduced as being 0.2 and only*
176 *in Section 3 a lengthy discussion of this value is given and sensitivity studies are performed. A*
177 *more thorough discussion of reasons and conditions of large or small $\Delta\kappa$,*
178 *respectively, should be added in the context of the applicability and accuracy of the new*
179 *method. How would the results change if not a constant $\Delta\kappa$ but the exact difference*
180 *for each data point in Fig 5 is used? Can we learn something from the resulting*
181 *(dis)agreement as a function of A?*

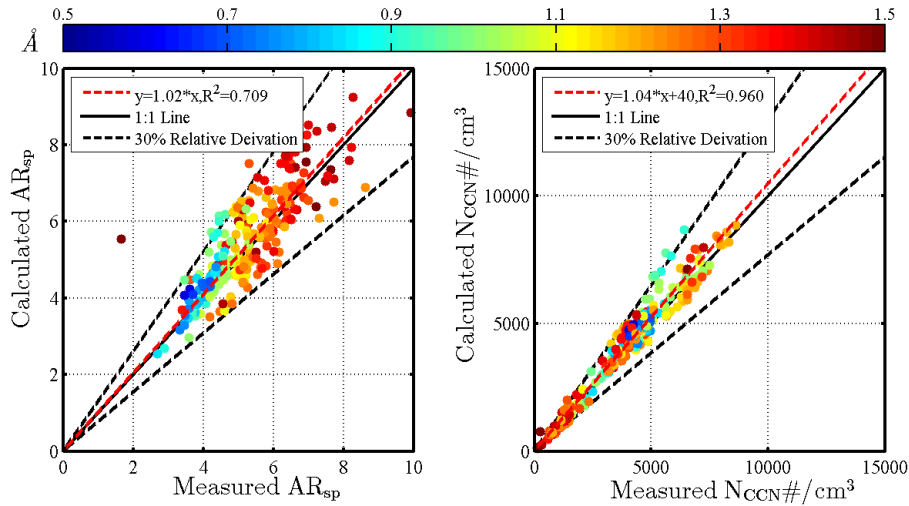
182 **Response:** Thanks for the suggestion.

183 We have added the discussion of reasons and conditions of $\Delta\kappa$ variations in the second to
184 last paragraph in Section 3 as follows:

185 *“...a smaller difference of 0.1 between κ_c and κ_f should be used (Kuang et al., 2017).*
186 *This simplified relationship between κ_c and κ_f is a rough estimate regardless of the*
187 *complexity of differences of aerosol hygroscopicity measured by different instruments, but still*
188 *used in this study for two reasons. First, the accurate conversion cannot be achieved without*
189 *detailed information of the particle hygroscopicity, which is difficult and complicated to*
190 *measure. Second, a deviation of κ_c less than 0.1 generally leads to a deviation of N_{CCN} less*
191 *than 20% (Ma et al., 2016), which is comparable with the deviation of CCN measurements.*
192 *As a result, for a simple method of N_{CCN} calculation, this conversion is quite easy. In addition,*
193 *it is important to note that the value of the difference between κ_c and κ_f is also a rough*
194 *estimate regardless of the complexity of aerosol hygroscopicity under different conditions, and*
195 *the influence of $\Delta\kappa$ deviation on N_{CCN} calculation needs to be further examined based on*
196 *field observation.”*

197 The use of exact $\Delta\kappa$ for each data point to calculate N_{CCN} means the application of
198 measured κ_c for N_{CCN} prediction based on the lookup table in Figure 2. This exclude the
199 uncertainty of aerosol hygroscopicity in predicting N_{CCN} and highlight the impact of PNSD's
200 variation on N_{CCN} prediction when \hat{A} is used to estimate the influence of PNSD on the
201 relationship between N_{CCN} and σ_{sp} . Calculated AR_{sp} and calculated N_{CCN} with corresponding
202 \hat{A} are shown in Figure S1. Relative deviations between calculated AR_{sp} and measured AR_{sp}
203 are generally no higher than 30%. Compared with correlations shown in the left plot of Figure
204 6, whose correlation coefficients ranges from 0.5 to 0.6, the correlation between calculated
205 AR_{sp} based on measured κ_c and measured AR_{sp} is better, with a correlation coefficient of
206 0.709. As for calculated N_{CCN} using measured κ_c , relative deviations are mainly within 30%.
207 Deviations of calculated AR_{sp} and calculated N_{CCN} are due to variations of PNSDs which

208 share a same \AA . In addition, as for relative deviations of both calculated AR_{sp} and calculated
 209 N_{CCN} , neither of them has a significant relationship with corresponding \AA . Besides the
 210 uncertainty of CCN measurement, causes of calculated N_{CCN} deviations also include
 211 variations of PNSDs with a common \AA are almost the same for different \AA , showing random
 212 fluctuations of PNSDs from their true values.



213
 214 Figure S1. Left plot: comparisons of calculated AR_{sp} based on measured κ_c and measured
 215 AR_{sp} . Right plot: regressions of calculated N_{CCN} based on measured κ_c and measured N_{CCN} .
 216 The color of the dot are corresponding \AA for each data point.

217
 218

219 6) *Formatting*

220 *All parameters should be expressed in equations and should be formatted and numbered*
 221 *as such. For example, l. 101 and the definition of fRH (l. 106).*

222 **Response:** Thanks for the suggestion. We have revised them accordingly.

223

224 7) *Figures*

225 *a) The caption of Figure 2 cannot be understood without reading the text. At the very least,*
 226 *the parameters should be spelled out and a reference to an equation in the text should be*
 227 *added.*

228 **Response:** Thanks for the suggestion. We have revised the caption as “Colors represent AR_{sp}

229 (calculated as $AR_{sp} = \frac{N_{CCN}}{\sigma_{sp}}$ at 450nm wavelength and 0.07% supersaturation) with different
 230 PNSDs (classified by \mathring{A} values) and different κ_c .”

231

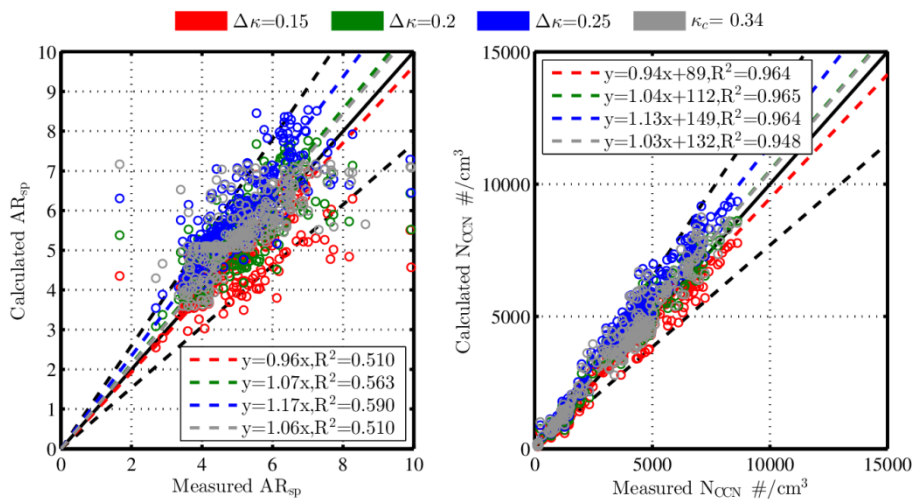
232 b) What are the grey bars in Figure 4?

233 **Response:** Thanks for the suggestion. The grey bars are periods when the sensitivity of
 234 AR_{sp} to κ_c is notable. We have added the description in the caption of Figure 4 and in the
 235 third paragraph of Section 3.2.

236

237 c) The grey symbols in Figure 6 overlap with many other symbols. Maybe choosing open
 238 symbols would improve clarity

239 **Response:** Thanks for the suggestion. We have revised Figure 6 as follows:



240

241

242 **Minor comments:**

243 l. 64: Add references for the ‘common use’.

244 **Response:** Thanks for the suggestion. We have added references as follows:

245 Jefferson, A.: Empirical estimates of CCN from aerosol optical properties at four remote
 246 sites, Atmos. Chem. Phys., 10, 6855-6861, 10.5194/acp-10-6855-2010, 2010.

247 Liu, J. J., and Li, Z. Q.: Estimation of cloud condensation nuclei concentration from
 248 aerosol optical quantities: influential factors and uncertainties, Atmospheric Chemistry and
 249 Physics, 14, 471-483, 10.5194/acp-14-471-2014, 2014.

250

251 *l. 66: This sentence needs work: 1) word missing after 'carbonaceous'. 2) What is meant*
252 *by 'most important hydrophobic'?*

253 **Response:** Thanks for the suggestion. The statement in the manuscript is confusing and
254 we have revised this sentence as: *"Black carbon dominates the absorption of solar radiation*
255 *and is a main hydrophobic composition as well."*

256

257 *l. 135/6: S is not included in the equation*

258 **Response:** Thanks for the suggestion. It should be RH and we have revised it accordingly.

259

260 *l. 164/5: Is this a result based on the literature or the current data set? If the former, add*
261 *references.*

262 **Response:** Thanks for the comment. It's based on literature and we have added references
263 as follows:

264 Cheng, Y. F., A. Wiedensohler, et al. (2008). "Aerosol optical properties and related
265 chemical apportionment at Xinken in Pearl River Delta of China." *Atmospheric Environment*
266 *42(25): 6351-6372.*

267 Ma, N., C. Zhao, et al. (2011). "Aerosol optical properties in the North China Plain during
268 HaChi campaign: an in-situ optical closure study." *Atmos. Chem. Phys* *11(12): 5959-5973.*

269 Liu, H. J., C. S. Zhao, et al. (2014). "Aerosol hygroscopicity derived from size-segregated
270 chemical composition and its parameterization in the North China Plain." *Atmos. Chem. Phys.*
271 *14(5): 2525-2539.*

272 Kuang, Y., C. S. Zhao, et al. (2017). "A novel method for deriving the aerosol
273 hygroscopicity parameter based only on measurements from a humidified nephelometer
274 system." *Atmospheric Chemistry and Physics* *17(11): 6651-6662.*

275

276 *l. 191: AR(sp) can only be 0 if N(CCN) or if sigma(sp) is infinitely large. Is either of this a*
277 *realistic situation?*

278 **Response:** Thanks for the suggestion. σ_{sp} wouldn't be infinitely large and AR_{sp} should be
279 higher than 0. We have revised it as: *"... and AR_{sp} is higher than 0 and lower than 10. ..."*

280

281 *l. 245: What ‘microphysical properties’ are you referring to here? ‘Composition’ is a*
282 *chemical property*

283 **Response:** Thanks for the comment. We are referring to the shape of particle size
284 distribution and aerosol hygroscopicity, and we have revised the last two sentences in this
285 paragraph as: “... *rather than the shape of particle size distribution and aerosol*
286 *hygroscopicity. Variations of AR_{sp} result from the variations of \dot{A} and κ_c , which indicate the*
287 *variations of aerosol microphysical properties and chemical compositions.*”

288

289 *l. 247: ‘more sensitive’ as compared to which other parameter?*

290 **Response:** Thanks for the comment. It should be κ_c and we have revised it accordingly.

291

292 *l. 249: Later and in Figure 2, the range of A is up to approx. 1.5, not 15*

293 **Response:** Thanks for the suggestion. We have revised it accordingly.

294

295 **Technical comments**

296 *l. 2: ‘Nuclei’ misspelled*

297 **Response:** Thanks for the suggestion. We have revised it.

298 *l. 94: an inlet . . . consisting of . . . an inline . . .*

299 **Response:** Thanks for the suggestion. We have revised them.

300 *l. 109: AR has not been defined before.*

301 **Response:** Thanks for the suggestion. We have revised it.

302 *l. 128: campaigns*

303 **Response:** Thanks for the suggestion. We have revised it.

304 *l. 154: indicates*

305 **Response:** Thanks for the suggestion. We have revised it.

306 *l. 159: wavelengths*

307 **Response:** Thanks for the suggestion. We have revised it.

308 *l. 171: increases*

309 **Response:** Thanks for the suggestion. We have revised it.

310 *l. 179: remove 'as'*

311 **Response:** Thanks for the suggestion. We have revised it.

312

313

314 **Reference:**

315 Wex, H., M. D. Petters, et al. (2009). "Towards closing the gap between hygroscopic growth and
316 activation for secondary organic aerosol: Part 1-Evidence from measurements." *Atmospheric
317 Chemistry and Physics* 9(12): 3987-3997.

318 Irwin, M., N. Good, et al. (2010). "Reconciliation of measurements of hygroscopic growth and
319 critical supersaturation of aerosol particles in central Germany." *Atmos. Chem. Phys.* 10(23):
320 11737-11752.

321 Good, N., D. O. Topping, et al. (2010). "Consistency between parameterisations of aerosol
322 hygroscopicity and CCN activity during the RHaMBLe discovery cruise." *Atmospheric Chemistry
323 and Physics* 10(7): 3189-3203.

324 Renbaum-Wolff, L., M. Song, et al. (2016). "Observations and implications of liquid–liquid
325 phase separation at high relative humidities in secondary organic material produced by α -pinene
326 ozonolysis without inorganic salts." *Atmos. Chem. Phys.* 16(12): 7969-7979.

327 Kuang, Y., C. S. Zhao, et al. (2017). "A novel method for deriving the aerosol hygroscopicity
328 parameter based only on measurements from a humidified nephelometer system." *Atmospheric
329 Chemistry and Physics* 17(11): 6651-6662.

330

A New Method for Calculating Number Concentrations of Cloud Condensation ~~Nuclei~~ Nuclei Based on Measurements of A Three-wavelength Humidified Nephelometer System

Jiangchuan Tao¹, Chunsheng Zhao¹, Ye Kuang¹, Gang Zhao¹, Chuanyang Shen¹, Yingli Yu¹, Yuxuan Bian², Wanyun Xu²

[1]{Department of Atmospheric and Oceanic Sciences, School of Physics, Peking University, Beijing, China}

[2]{State Key Laboratory of Severe Weather, Chinese Academy of Meteorological Sciences}

*Correspondence to: C. S. Zhao (zcs@pku.edu.cn)

Abstract

The number concentration of cloud condensation nuclei (CCN) plays a fundamental role in cloud physics. Instrumentations of direct measurements of CCN number concentration (N_{CCN}) based on chamber technology are complex and costly, thus a simple way for measuring N_{CCN} is needed. In this study, a new method for N_{CCN} calculation based on measurements of a three-wavelength humidified nephelometer system is proposed. A three-wavelength humidified nephelometer system can measure aerosol light scattering coefficient (σ_{sp}) at three wavelengths and the light scattering enhancement factor (fRH). The Angstrom exponent (\AA) inferred from σ_{sp} at three wavelengths provides information on mean predominate aerosol size and hygroscopicity parameter (κ) can be calculated from the combination of fRH and \AA . Given this, a look-up table that involves σ_{sp} , κ and \AA is established to predict N_{CCN} . Due to the precondition for the application, this new method is not suitable for externally mixed particles, large particles (e.g. dust and sea salt) or particles near single source regions. This method is validated with direct measurements of N_{CCN} using a CCN counter on the North China Plain. Results show that relative deviations between calculated N_{CCN} and measured N_{CCN} are within 30% and confirm the robustness of this method. This method enables simpler N_{CCN} measurements because the humidified nephelometer system is easily operated and stable. Compared

26 with the method of CCN counter, another advantage of this newly proposed method is that it can
27 obtain N_{CCN} at lower supersaturations in the ambient atmosphere.

28

29 1. Introduction

30 Cloud condensation nuclei (CCN) is the aerosol particle forming cloud droplet by hygroscopic
31 growth. CCN number concentration (N_{CCN}) plays a fundamental role in cloud micro physics and
32 aerosol indirect radiative effect. In general, the direct measurement of N_{CCN} is achieved in a cloud
33 chamber under super-saturated conditions (Hudson, 1989;Nenes et al., 2001;Rose et al., 2008). Due
34 to the requirement of high accuracies of working conditions like temperatures, vapors and flow rates
35 in cloud chambers, the direct measurement of N_{CCN} is complex and costly (Rose et al., 2008;Lathem
36 and Nenes, 2011). Thus, developments of simplified measurements of N_{CCN} are required. In recent
37 years, attention has been focused on measurements of aerosol optical properties (Jefferson,
38 2010;Ervens et al., 2007;Gasso and Hegg, 2003), which are simple and well-developed (Covert et al.,
39 1972;Titos et al., 2016). For aerosol population free of sea salt or dust, the accumulation mode
40 aerosol not only dominates aerosol scattering ability but also contribute most to N_{CCN} . Thus, the
41 calculation of N_{CCN} based on measurements of aerosol optical properties is feasible, and can facilitate
42 N_{CCN} measurement.

43 There are two kinds of methods to calculating N_{CCN} based on measurements of aerosol optical
44 properties. For the first kind, N_{CCN} as well as the hygroscopicity parameter (κ) can be calculated
45 based on measurements of a humidified nephelometer system in combination with aerosol particle
46 number size distribution (PNSD) (Ervens et al., 2007;Chen et al., 2014). Thus additional
47 measurements of PNSD are needed. For the second kind, N_{CCN} is calculated based on statistical
48 relationships between N_{CCN} and aerosol optical properties, such as scattering coefficient (σ_{sp}),
49 Angstrom Exponent (\AA , which is the exponent commonly used to describe the dependence of σ_{sp} on
50 wavelength) and single scattering albedo (SSA) (Jefferson, 2010;Shinozuka et al., 2015). Compared
51 with the first kind, whose R^2 can be about 0.9, instruments used in the second kind of methods are
52 cheaper and easier in operation, but has a lower accuracy of R^2 much lower than 0.9. Applications
53 similar to the second kind are widely used in remote sensing. As shown in Table 1, Earlier-earlier

54 studies found that the aerosol volume or aerosol PNSD retrieved from remote sensing measurements
55 can be used to calculate N_{CCN} (Gasso and Hegg, 2003; Kapustin et al., 2006). Recently, aerosol
56 optical depth (AOD) or aerosol vertical profile is used to predict N_{CCN} directly (Ghan and Collins,
57 2004; Ghan et al., 2006; Andreae, 2009; Liu and Li, 2014).

58 In the statistical relationship between N_{CCN} and aerosol optical properties, σ_{sp} or AOD is mainly
59 the proxy of aerosol absolute concentration, while \dot{A} or SSA can be used to reveal the variations of
60 aerosol CCN activity, as shown in Table 1. Based on Kohler theory (Köhler, 1936; Petters and
61 Kreidenweis, 2007), aerosol CCN activity is determined by aerosol size and aerosol chemical
62 composition which is defined as aerosol hygroscopicity. Information about aerosol size and aerosol
63 hygroscopicity are critical to N_{CCN} prediction and their absence can lead to a deviation with factor of
64 four (Andreae, 2009). Compared with aerosol hygroscopicity, aerosol size is more important in
65 determining CCN activity (Dusek et al., 2006). The value of \dot{A} can provide information on mean
66 predominate aerosol size (Brock et al., 2016; Kuang et al., 2017a). As a result, N_{CCN} calculation from
67 \dot{A} and extinction coefficient is found to be accurate to some extent (Shinozuka et al., 2015). As
68 proxies for aerosol hygroscopicity, SSA or aerosol light scattering enhancement factor (fRH) is
69 commonly used while not so effective (Jefferson, 2010; Liu and Li, 2014). SSA is determined by the
70 ratio between the light absorbing carbonaceous and less-absorbing components. Black carbon
71 dominates the absorption of solar radiation and is a main hydrophobic composition as well. Blaek
72 carbon contributes most to the light absorbing carbonaceous and is the most important hydrophobic
73 compositions as well. Less-absorbing components consist of inorganic salts and acids, as well as
74 most organic compounds, which are generally hygroscopic compositions. SSA correlates positively
75 with aerosol hygroscopicity (Rose et al., 2010) but deviates significantly due to the diversity of
76 hygroscopicity of less-absorbing components. Thus N_{CCN} calculation combining SSA, backscatter
77 fraction and σ_{sp} still lead to significant deviations, with a 0.6 R^2 (Jefferson, 2010). Thus deviations
78 of N_{CCN} calculation based on SSA is of large errors (Jefferson, 2010). As for fRH, there was a study
79 applied aerosol optical quantities (σ_{sp} or aerosol optical thickness) with fRH or SSA to calculate
80 N_{CCN} (Liu and Li, 2014). In their study, compared with the combination of SSA and aerosol optical
81 quantities, the combination of fRH and aerosol optical quantities is found to be less effective in

82 ~~estimating N_{CCN} , even though fRH directly connected with aerosol hygroscopicity (Liu and Li, 2014).~~
83 ~~Compared with SSA, previous studies found fRH to be less effective in estimating N_{CCN} , even~~
84 ~~though fRH directly connected with aerosol hygroscopicity (Liu and Li, 2014).~~ This may result from
85 the significant dependence of fRH on aerosol size (Chen et al., 2014; Kreidenweis and Asa-Awuku,
86 2014; Kuang et al., 2017a). As mentioned before, PNSD is used for better calculation of κ and N_{CCN}
87 from fRH in previous studies (Ervens et al., 2007; Chen et al., 2014). A new method to estimate κ
88 from fRH and \dot{A} was proposed recently (Kuang et al., 2017a; Brock et al., 2016). Based on this
89 method, fRH can be used to calculate N_{CCN} without measurements of PNSD and can be expected to
90 improve the N_{CCN} prediction just based on measurements of aerosol optical properties.

91 In this study, the relationship between N_{CCN} and aerosol optical properties measured by a
92 humidified nephelometer system is studied and a new method for N_{CCN} prediction is proposed. This
93 new method is validated based on data observed in Gucheng campaign on the North China Plain and
94 can be expected to improve measurements of N_{CCN} due to advantages of applying nephelometers.

96 2. Methodology

97 2.1. Data

98 Data in this study are mainly measured at Gucheng (39.15N, 115.74E) during autumn in 2016
99 on the North China Plain (NCP). Gucheng is 100km southwest from Beijing and 40km northeast
100 from Baoding under background pollution condition in the NCP. The observation site was
101 surrounded by farmland and about 3km away from the Gucheng town. This campaign started on 20
102 October and lasted for nearly one month.

103 Instruments used in Gucheng campaign were located in a measurement container under
104 temperature maintained at 25 °C. Ambient aerosol was sampled and dried to relative humidity (RH)
105 lower than 30% by an inlet system consisting of a PM10 inlet, an inline Nafion dryers and a RH and
106 temperature sensor (Vaisala HMP110). Then the sample aerosol was separated by a splitter and
107 directed into various instruments. During this campaign, aerosol scattering coefficient (σ_{sp}), aerosol
108 optical hygroscopic growth factor (fRH), particle size-resolved activation ratio (AR) and particle
109 number size distribution (PNSD) were obtained.

110 fRH as well as σ_{sp} at three wavelengths were measured by a humidified nephelometer system
111 consisting of two nephelometers (Aurora 3000, Ecotech Inc.) and a humidifier. σ_{sp} can be described
112 by a formula of Å:

$$113 \quad \sigma_{sp}(\lambda) = \beta \cdot \lambda^{-\text{Å}}, \quad (1)$$

114 where β is the aerosol number concentration and λ is the wavelength. Thus Å can be calculated
115 directly from σ_{sp} measured by a nephelometer. The humidifier with a Gore-Tex tube humidified the
116 sample air up to 90% RH. A whole cycle of humidification lasted about 45 minutes from 50% RH to
117 90% RH. Dried σ_{sp} was obtained directly from dried sample aerosol measured by one nephelometer
118 and humidified σ_{sp} was obtained from humidified aerosol measured by another nephelometer.

119 ~~fRH/RH~~ is defined as:

$$120 \quad fRH = \sigma_{sp}(RH) / \sigma_{sp} \quad (2)$$

121 ~~where $\sigma_{sp}(RH)$ is the humidified σ_{sp} at each RH, the ratio of the humidified σ_{sp} to the dried σ_{sp}~~
122 ~~at each RH.~~ Detailed description of the humidified nephelometer system was illustrated in Kuang et
123 al (2017a).

124 The particle size-resolved activation ratio (AR), defined as the ratio of N_{CCN} to total particles,
125 was measured by a system mainly consisting of a differential mobility analyzer (DMA, Model 3081)
126 and a continuous-flow CCN counter (model CCN200, Droplet Measurement Technologies, USA;
127 Roberts and Nenes (2005); Lance et al., (2006)). The system selected mono-disperse particles with
128 the DMA coupled with an electrostatic classifier (model 3080; TSI, Inc., Shoreview, MN USA) and
129 measured AR of the mono-disperse particles by a condensation particle counter (CPC model 3776;
130 TSI, Inc.) and CCN counter. Ranges of particle size and supersaturation were 10-300nm and
131 0.07%-0.80%, respectively. Measurements at five supersaturations (0.07%, 0.10%, 0.20%, 0.40%
132 and 0.80%) were conducted sequentially ~~and with~~ each cycle lasted for 1 hour, and N_{CCN} at 0.07%
133 supersaturation was used in this study. Before and after the campaign, supersaturations set in this
134 system were calibrated using ammonium sulfate (Rose et al., 2008). More information about the
135 system are given in Deng et al. (2011) and Ma et al. (2016).

136 PNSD with particle diameter from 9nm to 10um was measured by a mobility particle size

137 spectrometer (SMPS, TSI Inc., Model 3996) and an Aerodynamic Particle Sizer (APS, TSI Inc.,
 138 Model 3321). SMPS consisted of a DMA, an electrostatic classifier and a CPC (model 3776; TSI,
 139 Inc., Shoreview, MN USA) and measured PNSD with diameter lower than 700nm.

140 In addition, PNSD and σ_{sp} from 2011 to 2014 at four campaigns (Wuqing in 2011, Xianghe in
 141 2012 and 2013, and Wangdu in 2014) in NCP were used in this study. PNSD in these campaigns was
 142 measured by a Twin Differential Mobility Particle Sizer (TDMPMS, Leibniz-Institute for Tropospheric
 143 Research (IFT), Germany) and an Aerodynamic Particle Sizer (APS, TSI Inc., Model 3321). A TSI
 144 3563 nephelometer was used to obtain σ_{sp} at three wavelengths. Details about the four campaigns
 145 can be found in Ma et al. (2011), Ma et al.(2016), Kuang et al. (2016) and Kuang et al.(2017a).

146

147 2.2. Theories

148 Hygroscopic growth of particles at certain relative humidity can be described by κ -Köhler
 149 theory (Petters and Kreidenweis, 2007):

$$150 \quad \frac{RH}{100} = \frac{g(RH)^3 - 1}{g(RH)^3 - (1 - \kappa)} \cdot \exp\left(\frac{4\sigma_{s/a} \cdot M_w}{R \cdot T \cdot D_d \cdot g \cdot \rho_w}\right) \quad (1)$$

151 where $g(RH)$ is geometric diameter growth factor, κ is the hygroscopicity parameter, ~~S-RH~~ is
 152 the ~~saturation ratio~~ relative humidity; ρ_w is the density of water; M_w is the molecular weight of water;
 153 $\sigma_{s/a}$ is the surface tension of the solution–air interface, which is assumed to be equal to the surface
 154 tension of the pure water–air interface; R is the universal gas constant; and T is the temperature.

155 Accounting for the impact of \dot{A} , κ_f can be derived directly from fRH (Brock et al., 2016;Kuang
 156 et al., 2017a). A single-parameter parameterization scheme proposed by Brock et al. (2016) connects
 157 fRH and κ by the approximately proportional relationship between total aerosol volume and σ_{sp} :

$$158 \quad f(RH) = 1 + \kappa_{sca} \cdot RH / (100 - RH) \quad (2)$$

159 where κ_{sca} is a parameter for fitting fRH curves and is found can be used to predict κ_f in
 160 combination with \dot{A} in recent studies (Brock et al., 2016;Kuang et al., 2017a).~~can determines κ_f~~
 161 ~~with \dot{A} . This method of calculating κ_f based on κ_{sca} and \dot{A} was confirmed by good agreement~~
 162 with κ_f calculated from fRH and PNSD.~~This method was confirmed by good agreement with κ_f~~

163 | ~~calculated from f(RH) and g(RH)~~ (Brock et al., 2016;Kuang et al., 2017a).—

164 N_{CCN} can be calculated from size-resolved AR at a certain supersaturation (SS) and PNSD
165 (referred to as $n(\log D_p)$) as follows:

$$166 \quad N_{CCN} = \int_{\log D_p} AR(\log D_p, SS) \cdot n(\log D_p) d \log D_p \quad (3)$$

167 In general, size-resolved AR curves are complicated and always replaced by a critical diameter to
168 simplify calculation (Deng et al., 2013). The critical diameter is defined as:

$$169 \quad N_{CCN} = \int_{\log D_c}^{\log D_{p,max}} n(\log D_p) d \log D_p \quad (4)$$

170 where $D_{p,max}$ is the maximum diameter of the measured particle number size distribution. In other
171 words, the integral of PNSD larger than D_c equals to the measured N_{CCN} . And a critical κ (κ_c) can be
172 | calculated by equation (1) and ~~indicated-indicates~~ CCN activity and hygroscopicity of particles.

174 3. Results

175 3.1. Calculation of N_{CCN} based on measurements of a Humidified Nephelometer system

176 Free of sea salt aerosol and dust aerosol, accumulation mode aerosol dominates both the optical
177 | scattering ability at short wavelengths and the CCN activity at low supersaturationss, and thus a
178 reasonable relationship between σ_{sp} and N_{CCN} can be achieved. Figure 1 shows the size distribution
179 of cumulative contributions of σ_{sp} at 450nm and N_{CCN} at 0.07% with various \AA and κ_c , and
180 corresponding normalized PNSDs based on data measured at the four campaigns on the North China
181 Plain. During the four campaigns, no sea salt aerosol or dust aerosol was observed (Ma et al.,
182 2011;Ma et al., 2016;Kuang et al., 2016;Kuang et al., 2017a). For continental aerosol without sea salt
183 | or dust, \AA varies from 0.5 to 1.8 and κ_c varies from 0.1 to 0.5 (Cheng et al., 2008;Ma et al.,
184 2011;Liu et al., 2014;Kuang et al., 2017b). And as mentioned before, \AA can be used as a proxy of
185 the overall size distribution of aerosol populations, with smaller \AA indicating more larger particles.
186 | In figure 1, comparisons for \AA are made between 0.5 and ~~1.71.9~~ and for κ_c are made between 0.1
187 and 0.5. As larger particles contribute more to light scattering and activation, cumulative

188 contributions of both σ_{sp} and N_{CCN} increase significantly at the diameter range of accumulation
189 mode particles. Because more hygroscopic particles are able to activate at smaller diameters, the
190 cumulative contribution of N_{CCN} with higher κ_c increases at smaller diameters. In general, major
191 contributions of both σ_{sp} and N_{CCN} are made by particles from 200nm to 500nm for various \AA and
192 κ_c . This implies the feasibility of inferring N_{CCN} from aerosol optical properties.

193 Because particles smaller than 200nm can activate at supersaturations higher than 0.07% while
194 scatter less light at wavelengths longer than 450nm, which are shown as the light color lines in
195 Figure 1. Because smaller particles can activate at higher supersaturations while scatter less light at
196 longer wavelengths, it's obvious that significant differences will exist between cumulative
197 contributions of σ_{sp} and N_{CCN} . This means σ_{sp} and N_{CCN} are dominated by different particles and
198 poor correlation between σ_{sp} and N_{CCN} can be expected. Thus the method of inferring N_{CCN} from
199 aerosol optical properties is applicable for shorter wavelength and lower supersaturations.

200 Furthermore, PNSD with higher \AA indicates ~~as~~ more Aitken mode particles and fewer
201 accumulation mode particles. Thus large particles contribute less for both σ_{sp} and N_{CCN} when \AA are
202 higher, characterizing an increase of cumulative contribution curves at smaller diameters. In detail,
203 differences of cumulative contribution curves between 0.5 \AA and 1.9 \AA are about 150nm for σ_{sp}
204 and about 100nm for N_{CCN} , by estimating the average of differences of diameters where cumulative
205 contributions range from 0.2 to 0.8. ~~differences between cumulative contribution curves with \AA of~~
206 0.5 and 1.7 are about 150nm and 100nm for σ_{sp} and N_{CCN} , respectively. Changes of cumulative
207 contributions of N_{CCN} and σ_{sp} with various \AA reveal that the shape of PNSD can influence the
208 correlation between N_{CCN} and σ_{sp} . This is confirmed by previous studies in which the \AA is found to
209 play an important role in calculating N_{CCN} from σ_{sp} (Shinozuka et al., 2015; Liu and Li, 2014).

210 The relationship between σ_{sp} and N_{CCN} dependent on \AA and κ_c is evaluated by calculating
211 σ_{sp} and N_{CCN} with different PNSDs (classified by \AA) and different κ_c . In detail, ratios of N_{CCN} to

212 σ_{sp} , referred to as AR_{sp} , are calculated to eliminate the effect of variations of particle concentrations
213 consistent at all diameters. Results at the supersaturation of 0.07% are shown in figure 2 and AR_{sp} ~~is~~
214 ~~higher than 0 and lower than 10~~~~range from 0 to 10~~. In general, AR_{sp} are higher for more hygroscopic
215 particles or smaller particles. As particles become more hygroscopic, more CCN can be expected
216 when σ_{sp} is fixed. As aerosol populations consist of more smaller CCN-active particles, the increase
217 of σ_{sp} is weaker than that of N_{CCN} . For example, particles with diameters slightly larger than D_c
218 contribute less to σ_{sp} than particles with diameters much larger than D_c .

219 In detail, the sensitivity of AR_{sp} to \dot{A} also changes with \dot{A} and κ_c . When \dot{A} are higher than 1.4
220 and κ_c is lower than 0.2, AR_{sp} is insensitive to \dot{A} . While when \dot{A} are lower than 1 and κ_c are
221 higher than about 0.3, AR_{sp} is more sensitive to \dot{A} than κ_c . ~~Higher~~ This higher sensitivity of AR_{sp} to
222 \dot{A} ~~are found with higher κ_c and lower \dot{A} , which~~ reveals that particles having mean predominate size
223 smaller ~~more small particles and less large particles~~ than existing particles can contribute more to
224 N_{CCN} . This is the consequence of the sensitivity of AR_{sp} to \dot{A} resulting from the variation of small
225 CCN-active particles, as mentioned before.—

226 Based on the lookup-table illustrated in Figure 2, N_{CCN} at the supersaturation of 0.07% can be
227 calculated simply from \dot{A} , κ_f and σ_{sp} which can be obtained from measurements of a humidified
228 nephelometer system. The description of this simple method is shown in figure 3. A new look-up
229 table needs to be made for N_{CCN} estimation at other supersaturations, which should better be less than
230 0.07% as mentioned in the discussion of figure 1.

231 One critical issue about the method is the conversion of the κ_f obtained from the humidified
232 nephelometer system to the κ_c under super-saturated conditions. There are mainly two factors
233 making this conversion necessary. First, closure studies of aerosol hygroscopicity ~~found significant~~
234 deviations between hygroscopicity at sub-saturated conditions and super-saturated conditions (Wex
235 et al., 2009; Irwin et al., 2010; Good et al., 2010; Renbaum-Wolff et al. 2016). Their difference can
236 be expected to be about 0.1 for accumulation mode aerosol (Wu et al., 2013; Whitehead et al.,
237 2014; Ma et al., 2016). Second, ~~the~~ κ_f indicates the hygroscopicity of total particles and can be quite
238 different from aerosol hygroscopicity at a specific diameter due to variations of size distributions

239 ~~of size-dependent~~ particle hygroscopicity. Kuang et al. (2017a) found a difference around 0.1 between
240 κ_f and κ_c inferred from g(RH) measurements for accumulation mode particles whose κ_f is no larger
241 than 0.2. In this study, a simple conversion that κ_c is 0.2 higher than κ_f is used to calculate N_{CCN} ,
242 while for κ_f larger than 0.2, a smaller difference of 0.1 between κ_c and κ_f should be used (Kuang
243 et al., 2017a). This simplified relationship between κ_c and κ_f is a rough estimate regardless of the
244 complexity of differences of aerosol hygroscopicity measured by different instruments, but still used
245 in this study for two reasons~~is applicable for two reasons. On one hand~~First, the accurate conversion
246 cannot be achieved without detailed information of the particle hygroscopicity, which is difficult and
247 complicated to measure. ~~On the other hand~~Second, a deviation of κ_c less than 0.1 generally leads to
248 a deviation of N_{CCN} less than 20% (Ma et al., 2016), which is comparable with the deviation of CCN
249 measurements. As a result, for a simple method of N_{CCN} calculation, this conversion is quite easy ~~and~~
250 ~~adequate enough~~. In addition, it is important to note that the value of the difference between κ_c and
251 κ_f is also a rough estimate regardless of the complexity of aerosol hygroscopicity under different
252 conditions, and the influence of $\Delta\kappa$ deviation on N_{CCN} calculation needs to be further examined
253 based on field observation. In regions of single aerosol emissions or productions, the actual $\Delta\kappa$ can
254 be too large (some organic compositions, Wex et al., 2009; Renbaum-Wolff et al., 2016) or too small
255 (inorganic compositions and black carbon) and thus is not suitable for the application of this method.

256 Besides aerosol size and hygroscopicity, aerosol mixing state can also affect aerosol cloud
257 activity. When primary aerosol emissions are strong, aerosol populations are likely to be externally
258 mixed and a realistic treatment of aerosol mixing state is critical for N_{CCN} calculation (Cubison et al.,
259 2008; Wex et al., 2010). But for regions away from strong aerosol primary emissions, the influence of
260 mixing state on aerosol cloud activity is small and the assumption of internal mixing state is effective
261 for the estimation of N_{CCN} (Dusek et al., 2006; Deng et al., 2013; Ervens et al., 2010). For regions
262 above the boundary layer where clouds form and measurements of N_{CCN} are important, this
263 conclusion is tenable if there are no plumes (Moteki and Kondo, 2007; McMeeking et al., 2011). In
264 the new method of this paper aerosol populations are assumed to be internally mixed. Thus this
265 method might not be applicable for regions or air masses greatly affected by strong primary aerosol
266 emissions. Furthermore, this new method cannot be applied for regions where sea salt or dust
267 prevails, as mentioned before. In summary, this method can be used to calculate N_{CCN} for continental

268 regions, especially at clouds forming heights, where aged aerosol particles dominate.

269 3.2. Validation based on N_{CCN} measurement

270 The method for calculating N_{CCN} based on measurement of the humidified nephelometer system,
271 including the conversion of κ_c and the lookup-table, is examined using data measured in Gucheng.

272 Overview of data in Gucheng is shown in Figure 4. From polluted periods to clean periods,
273 significant variations of N_{CCN} and σ_{sp} can be found but AR_{sp} of N_{CCN} to σ_{sp} stays around 5. On
274 October 23rd and 29th, N_{CCN} and σ_{sp} are lower than $2000\#/cm^3$ and $500Mm^{-1}$, respectively. While on
275 October 20th, 26th and November 3rd, N_{CCN} and σ_{sp} are higher than $2000\#/cm^3$ and $500Mm^{-1}$,
276 respectively. These variations of N_{CCN} and σ_{sp} are mainly due to the variation of the particle number
277 concentration rather than ~~the shape of particle size distribution and aerosol hygroscopicity~~
278 ~~the particle microphysical properties~~. Variations of AR_{sp} result from the variations of \mathring{A} and κ_c , which indicate
279 the variations of aerosol microphysical properties and chemical compositions.

280 In general, AR_{sp} is more sensitive to variations of \mathring{A} than κ_c . As mentioned before, the
281 sensitivity of AR_{sp} to \mathring{A} is determined by both \mathring{A} and κ_f . In detail, \mathring{A} during the campaign mainly
282 ranges from 0.5 to ~~1.5~~ 1.5 and κ_f ranges mainly from 0.05 to 0.2, which means that κ_c ranges from
283 0.25 to 0.4. These values of \mathring{A} and κ_f correspond a significant sensitivity of AR_{sp} to \mathring{A} , as the
284 lookup table shows in figure 2. The sensitivity of AR_{sp} to κ_c is much small and only notable during
285 some short periods (grey bars in Figure 4). For example, from November 5th to 7th, variations of κ_f
286 and \mathring{A} are opposite and result in nearly constant AR_{sp} . And from October 30th to November 2nd,
287 consistent variations of \mathring{A} and κ_f lead to greater variations of AR_{sp} than other periods. This weak
288 sensitivity of AR_{sp} to κ_f may be due to the uncertainty of κ_c calculated from κ_f based on the
289 simplified conversion.

290 This simplified conversion of κ_c is examined by comparing κ_f and κ_c measured in Gucheng
291 campaign, shown in Figure 5. In general, $\Delta\kappa$ that indicates the difference between κ_f and κ_c is
292 around 0.2 and independent from \mathring{A} and κ_c . Over 80% of $\Delta\kappa$ ranges from 0.1 to 0.3 that confirms
293 applicability of the simplified conversion of κ_c . However, a notable deviation of $\Delta\kappa$ can be found
294 when \mathring{A} is higher than 1.5. High values of \mathring{A} represent existence of small particles. Compositions

295 and mixing state of these small particles, which may be fresh emitted and experience inefficient
296 aging processes, are diverse and likely to deviate from the simplified conversion of κ_c .

297 Therefore, considering the deviation of κ_c conversion and high sensitivity of AR_{sp} to κ_c when
298 \dot{A} is higher than 1.5, the method of calculating N_{CCN} from measurements of a humidified
299 nephelometer system may lead to significant deviation in this case which means that this method can
300 only be adopted when \dot{A} is lower than 1.5.

301 Based on the lookup table of κ_c and \dot{A} , AR_{sp} is calculated and applied to calculate N_{CCN} with
302 σ_{sp} . The calculated AR_{sp} and N_{CCN} are compared with the measured AR_{sp} and N_{CCN} shown as the
303 green dots in Figure 6. In general, good agreements between calculations and measurements are
304 achieved and relative deviations are within 30%. For the comparison of AR_{sp} , the system relative
305 deviation is less than 10%. For the comparison of N_{CCN} , the slope and the correlation coefficient of
306 the regression are 1.03 and 0.966, respectively.

307 In addition, the influence of the κ_c conversion on AR_{sp} and N_{CCN} calculation are evaluated in
308 two ways. In the first way, $\Delta\kappa$ of the κ_c conversion is set to be 0.05 higher or lower, which means
309 $\Delta\kappa$ of 0.25 or 0.15. The corresponding results are presented as the red dots and blue dots in Figure 6.
310 In the second way, a constant κ_c of 0.34, which is the average of κ_c values in Gucheng campaign,
311 is used to calculate AR_{sp} and N_{CCN} , and shown as the grey dots in Figure 6. In general, differences
312 among calculations using various κ_c conversions are quite small. The $\Delta\kappa$ difference of 0.05 in κ_c
313 conversion only leads to a difference of 10% for the system relative deviation. The correlation
314 coefficient of the calculation using a constant κ_c is just a little lower than correlation coefficients of
315 calculations using a κ_c conversion. As a result, the method of calculating N_{CCN} is insensitive to the
316 uncertainty of the κ_c conversion.

317 In this study, the insensitivity of calculated N_{CCN} to κ_c conversion is partly due to the small
318 variation of κ_f during the campaign. On one hand, the variation of κ_c can be quite large and cause
319 non-ignorable deviations of calculated N_{CCN} . As previous studies of N_{CCN} measurement showed, the
320 variation of κ_c is often small and a constant κ_c can be used to calculate N_{CCN} accurately (Andreae
321 and Rosenfeld, 2008; Gunthe et al., 2009; Rose et al., 2010; Deng et al., 2013). Results in this study
322 are similar to these previous studies. However, large variations of κ_c are also found in some other

323 studies. In NCP, fluctuations of aerosol hygroscopicity during New Particle Formation events and
324 soot emissions lead to significant deviations of calculated N_{CCN} from average aerosol hygroscopicity
325 (Ma et al., 2016). On the other hand, the influence of κ_c cannot be ignored because the value of the
326 average hygroscopicity is different in various regions during various periods. In summer of NCP,
327 measured κ_f at sub-saturated conditions can reach up to 0.45 when inorganic compositions
328 dominate in particles (Kuang et al., 2016). In this case, calculated N_{CCN} ignoring κ_c may be 10 times
329 larger than measured N_{CCN} . To sum up, although the exact value of κ_c cannot be obtained from the
330 measurement of the humidified nephelometer system, the influence of κ_c on N_{CCN} can be inferred
331 and is found to be correct enough considering the convenience of this method. More data, especially
332 in observations of more hygroscopic aerosol, is still needed to confirm this method.

333 4. Conclusions

334 N_{CCN} is a key parameter of cloud microphysics and aerosol indirect radiative effect. Direct
335 measurements of N_{CCN} are generally conducted under super-saturated conditions in cloud chambers,
336 and are complex and costly. The aerosols of accumulation mode contribute most to both the aerosol
337 scattering coefficient and the aerosol CCN activity. In view of this, it is possible to predict N_{CCN}
338 based on relationships between aerosol optical properties and the aerosol CCN activity. In this study,
339 a new method is proposed to calculate N_{CCN} based on measurements of a humidified nephelometer
340 system. In this method, N_{CCN} is derived from a look-up table which involves σ_{sp} , \dot{A} and κ_f , and
341 the required three parameters can be obtained from a three-wavelength humidified nephelometer
342 system.

343 Relationships between aerosol optical properties and aerosol CCN activity are investigated using
344 datasets about aerosol PNSD measured during several campaigns in the North China Plain. The
345 relationship between σ_{sp} , \dot{A} , κ_c and N_{CCN} is analyzed. It is found that the ratio between N_{CCN} and
346 σ_{sp} , referred to as AR_{sp} , is determined by κ_c and \dot{A} . In light of this, it is possible to calculate N_{CCN}
347 based only on measurements of a three-wavelength humidified nephelometer system which provides
348 information about σ_{sp} , the hygroscopicity parameter κ and \dot{A} . —However, κ derived from
349 measurements of a humidified nephelometer system under sub-saturated conditions (termed as κ_f)

350 differs from κ under super-saturated conditions which indicate CCN activity (termed as κ_c). As a
351 result, the conversion from κ_f to κ_c is needed. Based on previous studies of aerosol hygroscopicity
352 and CCN activity, a simple conversion from κ_f to κ_c with a fixed difference (referred to as $\Delta\kappa$) of
353 0.2 is proposed. On the basis of this simple conversion, the method of N_{CCN} prediction based only on
354 measurements of a humidified nephelometer system is achieved under conditions without sea salt
355 aerosol, ~~or~~ dust aerosol, externally mixed aerosol or aerosol near single source regions.

356 This method is validated with measurements from a humidified nephelometer system and a CCN
357 counter in Gucheng in 2016. During the campaign, both N_{CCN} and σ_{sp} vary with the pollution
358 conditions. AR_{sp} is around 5 and changes with \AA and κ_f . The difference between κ_f and κ_c , ~~was~~
359 0.2 ± 0.1 . The agreement between the calculated N_{CCN} and the measured N_{CCN} is achieved with
360 relative deviations less than 30%. Sensitivity of calculated N_{CCN} to conversions from κ_f to κ_c is
361 studied by applying different kinds of conversions. Results show that calculated N_{CCN} varies little
362 and is insensitive to the conversions, which confirms the robustness and applicability of this newly
363 proposed method.

364 This study has connected aerosol optical properties with N_{CCN} , and also proposed a novel
365 method to calculate N_{CCN} based only on measurements of a three-wavelength humidified
366 nephelometer system. Due to the simple operation and stability of the humidified nephelometer
367 system, this method will facilitate the real time monitoring of N_{CCN} , especially on aircrafts. In
368 addition, measurements of the widely used CCN counter are limited to supersaturations higher than
369 0.07. This method is more suitable for calculating N_{CCN} at lower supersaturations, thus is more
370 applicable for ambient measurements of clouds and fogs in the atmosphere.

371

372 Acknowledgement

373 This work is supported by the National Natural Science Foundation of China (41590872,
374 41375134 and 41505107).

375

376 Reference

- 377 Andreae, M. O., and Rosenfeld, D.: Aerosol-cloud-precipitation interactions. Part 1. The nature and sources of cloud-active aerosols,
378 Earth-Science Reviews, 89, 13-41, 10.1016/j.earscirev.2008.03.001, 2008.
- 379 Andreae, M. O.: Correlation between cloud condensation nuclei concentration and aerosol optical thickness in remote and polluted
380 regions, Atmospheric Chemistry and Physics, 9, 543-556, 2009.
- 381 Brock, C. A., Wagner, N. L., Anderson, B. E., Attwood, A. R., Beyersdorf, A., Campuzano-Jost, P., Carlton, A. G., Day, D. A., Diskin, G. S.,
382 Gordon, T. D., Jimenez, J. L., Lack, D. A., Liao, J., Markovic, M. Z., Middlebrook, A. M., Ng, N. L., Perring, A. E., Richardson, M. S.,
383 Schwarz, J. P., Washenfelder, R. A., Welti, A., Xu, L., Ziemba, L. D., and Murphy, D. M.: Aerosol optical properties in the southeastern
384 United States in summer – Part 1: Hygroscopic growth, Atmos. Chem. Phys., 16, 4987-5007, 10.5194/acp-16-4987-2016, 2016.
- 385 Chen, J., Zhao, C. S., Ma, N., and Yan, P.: Aerosol hygroscopicity parameter derived from the light scattering enhancement factor
386 measurements in the North China Plain, Atmos. Chem. Phys., 14, 8105-8118, 10.5194/acp-14-8105-2014, 2014.
- 387 Cheng, Y. F., Wiedensohler, A., Eichler, H., Su, H., Gnauk, T., Brueggemann, E., Herrmann, H., Heintzenberg, J., Slanina, J., Tuch, T., Hu,
388 M., and Zhang, Y. H.: Aerosol optical properties and related chemical apportionment at Xinken in Pearl River Delta of China, Atmos.
389 Environ., 42, 6351-6372, 10.1016/j.atmosenv.2008.02.034, 2008.
- 390 Covert, D. S., Charlson, R., and Ahlquist, N.: A study of the relationship of chemical composition and humidity to light scattering by
391 aerosols, Journal of applied meteorology, 11, 968-976, 1972.
- 392 Cubison, M. J., Ervens, B., Feingold, G., Docherty, K. S., Ulbrich, I. M., Shields, L., Prather, K., Hering, S., and Jimenez, J. L.: The
393 influence of chemical composition and mixing state of Los Angeles urban aerosol on CCN number and cloud properties, Atmospheric
394 Chemistry and Physics, 8, 5649-5667, 2008.
- 395 Deng, Z. Z., Zhao, C. S., Ma, N., Liu, P. F., Ran, L., Xu, W. Y., Chen, J., Liang, Z., Liang, S., Huang, M. Y., Ma, X. C., Zhang, Q., Quan, J. N.,
396 Yan, P., Henning, S., Mildenerger, K., Sommerhage, E., Schäfer, M., Stratmann, F., and Wiedensohler, A.: Size-resolved and bulk
397 activation properties of aerosols in the North China Plain, Atmos. Chem. Phys., 11, 3835-3846, 10.5194/acp-11-3835-2011, 2011.
- 398 Deng, Z. Z., Zhao, C. S., Ma, N., Ran, L., Zhou, G. Q., Lu, D. R., and Zhou, X. J.: An examination of parameterizations for the CCN
399 number concentration based on in situ measurements of aerosol activation properties in the North China Plain, Atmos. Chem. Phys.,
400 13, 6227-6237, 10.5194/acp-13-6227-2013, 2013.
- 401 Dusek, U., Frank, G., Hildebrandt, L., Curtius, J., Schneider, J., Walter, S., Chand, D., Drewnick, F., Hings, S., and Jung, D.: Size matters
402 more than chemistry for cloud-nucleating ability of aerosol particles, Science, 312, 1375-1378, 2006.
- 403 Ervens, B., Cubison, M., Andrews, E., Feingold, G., Ogren, J. A., Jimenez, J. L., DeCarlo, P., and Nenes, A.: Prediction of cloud
404 condensation nucleus number concentration using measurements of aerosol size distributions and composition and light scattering
405 enhancement due to humidity, Journal of Geophysical Research: Atmospheres, 112, n/a-n/a, 10.1029/2006jd007426, 2007.
- 406 Ervens, B., Cubison, M. J., Andrews, E., Feingold, G., Ogren, J. A., Jimenez, J. L., Quinn, P. K., Bates, T. S., Wang, J., Zhang, Q., Coe, H.,
407 Flynn, M., and Allan, J. D.: CCN predictions using simplified assumptions of organic aerosol composition and mixing state: a synthesis
408 from six different locations, Atmospheric Chemistry and Physics, 10, 4795-4807, 10.5194/acp-10-4795-2010, 2010.
- 409 Gasso, S., and Hegg, D. A.: On the retrieval of columnar aerosol mass and CCN concentration by MODIS, J. Geophys. Res.-Atmos., 108,
410 4010
411 10.1029/2002jd002382, 2003.
- 412 Ghan, S. J., and Collins, D. R.: Use of in situ data to test a Raman lidar-based cloud condensation nuclei remote sensing method,
413 Journal of Atmospheric and Oceanic Technology, 21, 387-394, 10.1175/1520-0426(2004)021<0387:uoisdt>2.0.co;2, 2004.
- 414 Ghan, S. J., Rissman, T. A., Elleman, R., Ferrare, R. A., Turner, D., Flynn, C., Wang, J., Ogren, J., Hudson, J., Jonsson, H. H., VanReken, T.,
415 Flagan, R. C., and Seinfeld, J. H.: Use of in situ cloud condensation nuclei, extinction, and aerosol size distribution measurements to
416 test a method for retrieving cloud condensation nuclei profiles from surface measurements, J. Geophys. Res.-Atmos., 111, D05s10
417 10.1029/2004jd005752, 2006.
- 418 Gunthe, S. S., King, S. M., Rose, D., Chen, Q., Roldin, P., Farmer, D. K., Jimenez, J. L., Artaxo, P., Andreae, M. O., Martin, S. T., and Poschl,
419 U.: Cloud condensation nuclei in pristine tropical rainforest air of Amazonia: size-resolved measurements and modeling of

420 atmospheric aerosol composition and CCN activity, *Atmospheric Chemistry and Physics*, 9, 7551-7575, 2009.

421 Hudson, J. G.: AN INSTANTANEOUS CCN SPECTROMETER, *Journal of Atmospheric and Oceanic Technology*, 6, 1055-1065,
422 10.1175/1520-0426(1989)006<1055:aics>2.0.co;2, 1989.

423 Jefferson, A.: Empirical estimates of CCN from aerosol optical properties at four remote sites, *Atmos. Chem. Phys.*, 10, 6855-6861,
424 10.5194/acp-10-6855-2010, 2010.

425 Köhler, H.: The nucleus in and the growth of hygroscopic droplets, *Transactions of the Faraday Society*, 32, 1152-1161, 1936.

426 Kapustin, V. N., Clarke, A. D., Shinozuka, Y., Howell, S., Brekhovskikh, V., Nakajima, T., and Higurashi, A.: On the determination of a
427 cloud condensation nuclei from satellite: Challenges and possibilities, *J. Geophys. Res.-Atmos.*, 111, D04202
428 10.1029/2004jd005527, 2006.

429 Kreidenweis, S. M., and Asa-Awuku, A.: 5.13 - Aerosol Hygroscopicity: Particle Water Content and Its Role in Atmospheric Processes
430 A2 - Holland, Heinrich D, in: *Treatise on Geochemistry (Second Edition)*, edited by: Turekian, K. K., Elsevier, Oxford, 331-361, 2014.

431 Kuang, Y., Zhao, C. S., Ma, N., Liu, H. J., Bian, Y. X., Tao, J. C., and Hu, M.: Deliquescent phenomena of ambient aerosols on the North
432 China Plain, *Geophys. Res. Lett.*, n/a-n/a, 10.1002/2016gl070273, 2016.

433 Kuang, Y., Zhao, C., Tao, J., Bian, Y., Ma, N., and Zhao, G.: A novel method to derive the aerosol hygroscopicity parameter based only
434 on measurements from a humidified nephelometer system, *Atmos. Chem. Phys. Discuss.*, 2017, 1-25, 10.5194/acp-2016-1066, 2017a.

435 Kuang, Y., Zhao, C. S., Tao, J. C., Bian, Y. X., Ma, N., and Zhao, G.: A novel method for deriving the aerosol hygroscopicity parameter
436 based only on measurements from a humidified nephelometer system, *Atmospheric Chemistry and Physics*, 17, 6651-6662,
437 10.5194/acp-17-6651-2017, 2017b.

438 Lance, S., Nenes, A., Medina, J., and Smith, J.: Mapping the operation of the DMT continuous flow CCN counter, *Aerosol science and
439 technology*, 40, 242-254, 2006.

440 Lathem, T. L., and Nenes, A.: Water Vapor Depletion in the DMT Continuous-Flow CCN Chamber: Effects on Supersaturation and
441 Droplet Growth, *Aerosol science and technology*, 45, 604-615, 10.1080/02786826.2010.551146, 2011.

442 Liu, H. J., Zhao, C. S., Nekat, B., Ma, N., Wiedensohler, A., van Pinxteren, D., Spindler, G., Müller, K., and Herrmann, H.: Aerosol
443 hygroscopicity derived from size-segregated chemical composition and its parameterization in the North China Plain, *Atmos. Chem.
444 Phys.*, 14, 2525-2539, 10.5194/acp-14-2525-2014, 2014.

445 Liu, J. J., and Li, Z. Q.: Estimation of cloud condensation nuclei concentration from aerosol optical quantities: influential factors and
446 uncertainties, *Atmospheric Chemistry and Physics*, 14, 471-483, 10.5194/acp-14-471-2014, 2014.

447 Ma, N., Zhao, C., Nowak, A., Müller, T., Pfeifer, S., Cheng, Y., Deng, Z., Liu, P., Xu, W., and Ran, L.: Aerosol optical properties in the
448 North China Plain during HaChi campaign: an in-situ optical closure study, *Atmos. Chem. Phys.*, 11, 5959-5973, 2011.

449 Ma, N., Zhao, C., Tao, J., Wu, Z., Kecorius, S., Wang, Z., Größ, J., Liu, H., Bian, Y., Kuang, Y., Teich, M., Spindler, G., Müller, K., van
450 Pinxteren, D., Herrmann, H., Hu, M., and Wiedensohler, A.: Variation of CCN activity during new particle formation events in the
451 North China Plain, *Atmos. Chem. Phys.*, 16, 8593-8607, 10.5194/acp-16-8593-2016, 2016.

452 McMeeking, G. R., Morgan, W. T., Flynn, M., Highwood, E. J., Turnbull, K., Haywood, J., and Coe, H.: Black carbon aerosol mixing state,
453 organic aerosols and aerosol optical properties over the United Kingdom, *Atmos. Chem. Phys.*, 11, 9037-9052,
454 10.5194/acp-11-9037-2011, 2011.

455 Moteki, N., and Kondo, Y.: Effects of Mixing State on Black Carbon Measurements by Laser-Induced Incandescence, *Aerosol science
456 and technology*, 41, 398-417, 10.1080/02786820701199728, 2007.

457 Nenes, A., Chuang, P. Y., Flagan, R. C., and Seinfeld, J. H.: A theoretical analysis of cloud condensation nucleus (CCN) instruments, *J.
458 Geophys. Res.-Atmos.*, 106, 3449-3474, 10.1029/2000jd900614, 2001.

459 Petters, M. D., and Kreidenweis, S. M.: A single parameter representation of hygroscopic growth and cloud condensation nucleus
460 activity, *Atmospheric Chemistry and Physics*, 7, 1961-1971, 2007.

461 Roberts, G., and Nenes, A.: A continuous-flow streamwise thermal-gradient CCN chamber for atmospheric measurements, *Aerosol
462 science and technology*, 39, 206-221, 2005.

463 Rose, D., Gunthe, S., Mikhailov, E., Frank, G., Dusek, U., Andreae, M., and Pöschl, U.: Calibration and measurement uncertainties of a

464 continuous-flow cloud condensation nuclei counter (DMT-CCNC): CCN activation of ammonium sulfate and sodium chloride aerosol
465 particles in theory and experiment, *Atmospheric Chemistry and Physics*, 8, 1153-1179, 2008.

466 Rose, D., Nowak, A., Achtert, P., Wiedensohler, A., Hu, M., Shao, M., Zhang, Y., Andreae, M. O., and Poschl, U.: Cloud condensation
467 nuclei in polluted air and biomass burning smoke near the mega-city Guangzhou, China - Part 1: Size-resolved measurements and
468 implications for the modeling of aerosol particle hygroscopicity and CCN activity, *Atmospheric Chemistry and Physics*, 10, 3365-3383,
469 2010.

470 Shinozuka, Y., Clarke, A. D., Nenes, A., Jefferson, A., Wood, R., McNaughton, C. S., Ström, J., Tunved, P., Redemann, J., Thornhill, K. L.,
471 Moore, R. H., Latham, T. L., Lin, J. J., and Yoon, Y. J.: The relationship between cloud condensation nuclei (CCN) concentration and light
472 extinction of dried particles: indications of underlying aerosol processes and implications for satellite-based CCN estimates, *Atmos.*
473 *Chem. Phys.*, 15, 7585-7604, 10.5194/acp-15-7585-2015, 2015.

474 Titos, G., Cazorla, A., Zieger, P., Andrews, E., Lyamani, H., Granados-Muñoz, M. J., Olmo, F. J., and Alados-Arboledas, L.: Effect of
475 hygroscopic growth on the aerosol light-scattering coefficient: A review of measurements, techniques and error sources, *Atmos.*
476 *Environ.*, 141, 494-507, <http://dx.doi.org/10.1016/j.atmosenv.2016.07.021>, 2016.

477 Wex, H., McFiggans, G., Henning, S., and Stratmann, F.: Influence of the external mixing state of atmospheric aerosol on derived CCN
478 number concentrations, *Geophys. Res. Lett.*, 37, L10805
479 10.1029/2010gl043337, 2010.

480 Whitehead, J. D., Irwin, M., Allan, J. D., Good, N., and McFiggans, G.: A meta-analysis of particle water uptake reconciliation studies,
481 *Atmos. Chem. Phys.*, 14, 11833-11841, 10.5194/acp-14-11833-2014, 2014.

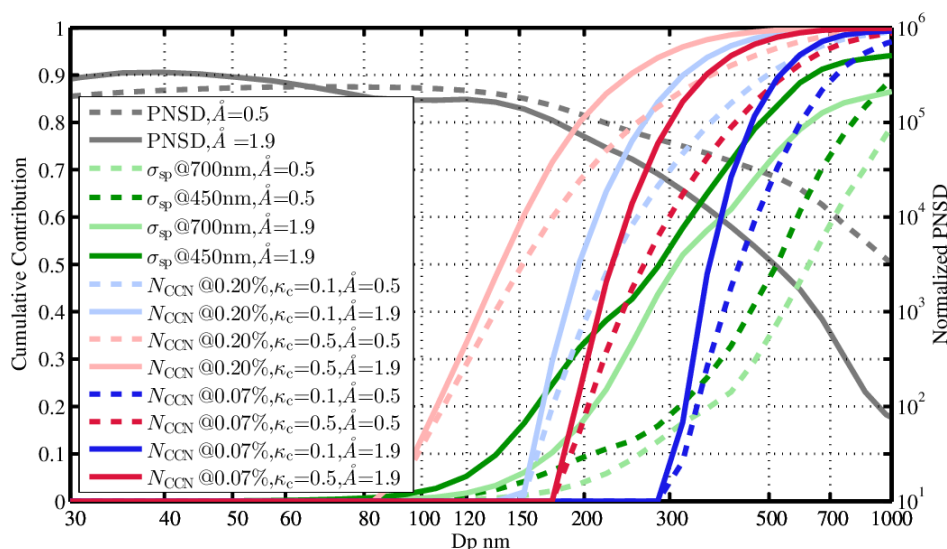
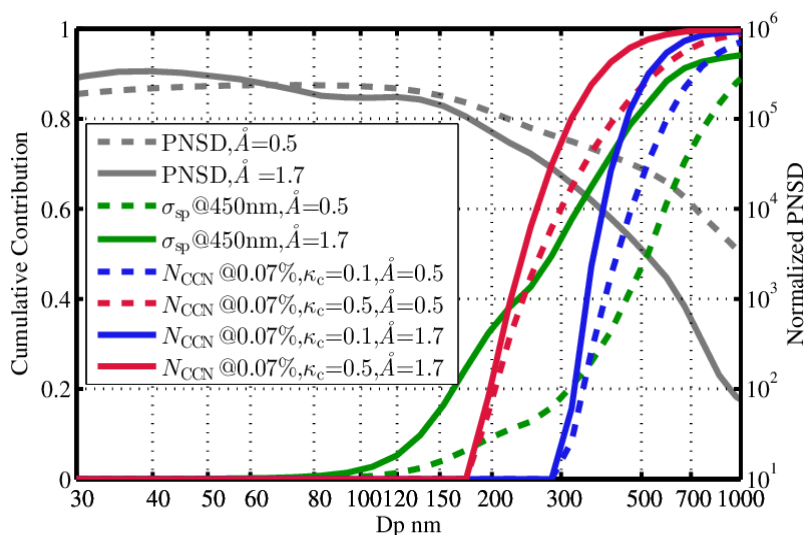
482 Wu, Z. J., Poulain, L., Henning, S., Dieckmann, K., Birmili, W., Merkel, M., van Pinxteren, D., Spindler, G., Mueller, K., Stratmann, F.,
483 Herrmann, H., and Wiedensohler, A.: Relating particle hygroscopicity and CCN activity to chemical composition during the HCCT-2010
484 field campaign, *Atmospheric Chemistry and Physics*, 13, 7983-7996, 10.5194/acp-13-7983-2013, 2013.

485 [Renbaum-Wolff, L., M. Song, et al. \(2016\). "Observations and implications of liquid-liquid phase separation at high relative
486 humidities in secondary organic material produced by \$\alpha\$ -pinene ozonolysis without inorganic salts." *Atmos. Chem. Phys.*
487 *16\(12\): 7969-7979.*](#)

488 [Irwin, M., N. Good, et al. \(2010\). "Reconciliation of measurements of hygroscopic growth and critical supersaturation of
489 aerosol particles in central Germany." *Atmos. Chem. Phys.* **10\(23\): 11737-11752.**](#)

490 [Good, N., D. O. Topping, et al. \(2010\). "Consistency between parameterisations of aerosol hygroscopicity and CCN activity
491 during the RHaMBLe discovery cruise." *Atmospheric Chemistry and Physics* **10\(7\): 3189-3203.**](#)

492

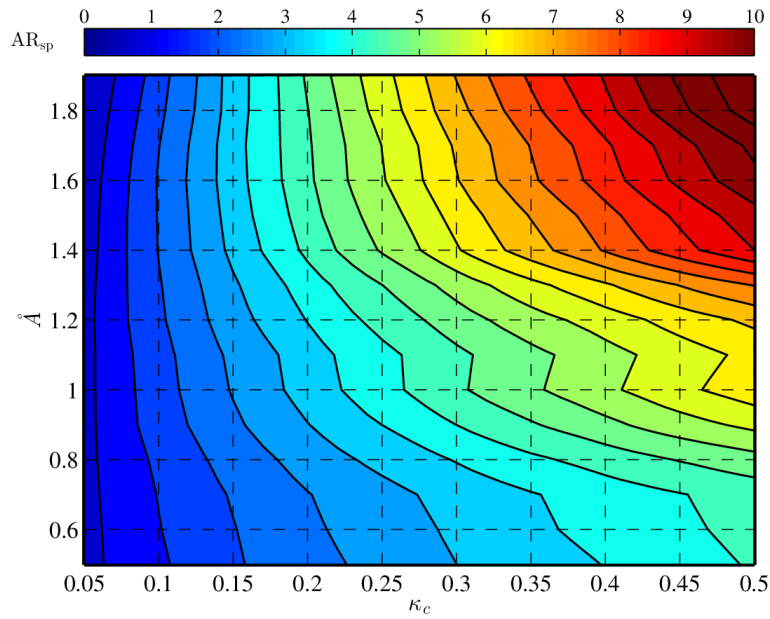


493

494

495 Figure 1.

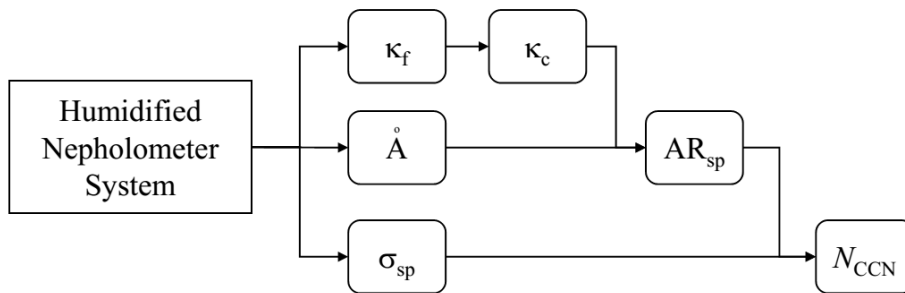
496 Aerosol PNSD (black lines), the cumulative contribution of σ_{sp} at wavelength of 450nm and 700nm
 497 (dark green lines and light green lines, respectively green lines), and the cumulative contribution of
 498 N_{CCN} at supersaturation of 0.07% (dark red and dark blue lines red and blue lines) and the cumulative
 499 contribution of N_{CCN} at supersaturation of 0.20% (light red and light blue lines) based on
 500 measurement in several campaigns in the North China Plain. Solid lines and dashed lines indicate \dot{A}
 501 of 1.7, 1.9 and 0.5, respectively. Blue lines and red lines indicate κ_c of 0.1 and 0.5, respectively.



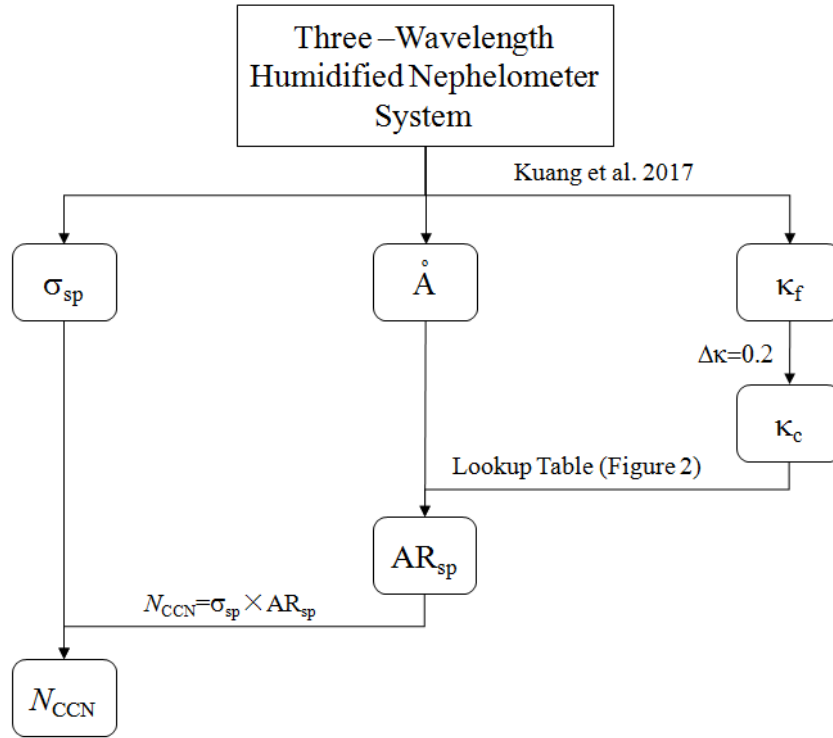
502

503 Figure 2.

504 Colors represent AR_{sp} (calculated as $AR_{sp} = \frac{N_{CCN}}{\sigma_{sp}}$ at 450nm wavelength and 0.07% supersaturation)
 505 with different PNSDs (classified by \tilde{A} values) and different κ_c . Colors represent AR_{sp} (ratios
 506 between N_{CCN} and σ_{sp}) with κ_c and \tilde{A} .



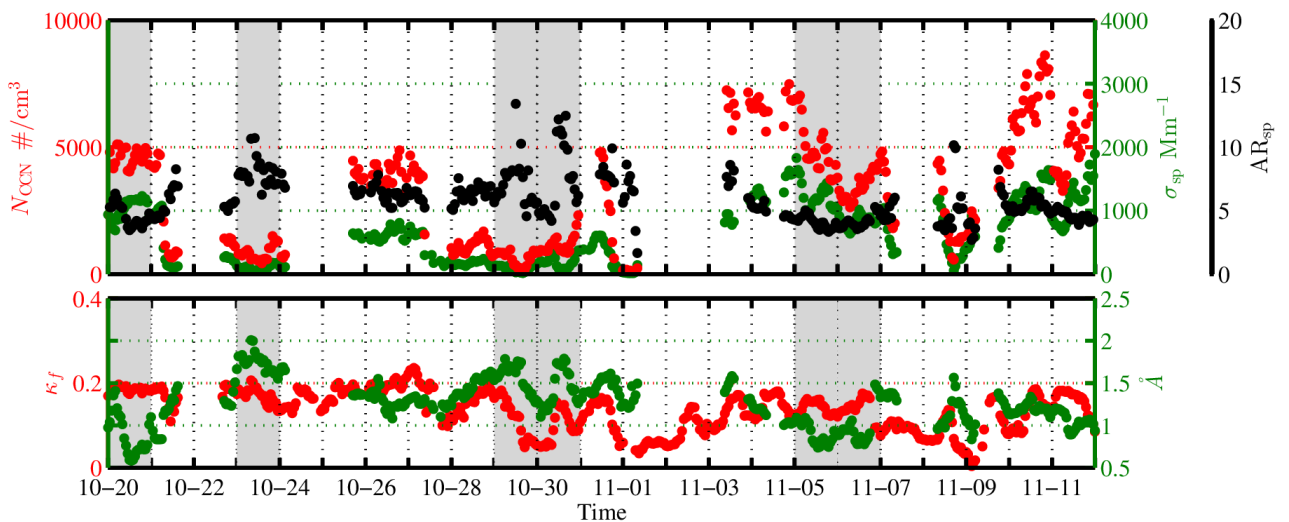
507



508

509 Figure 3.

510 The schematic chart of the N_{CCN} prediction based on measurements of a humidified nephelometer
 511 system.

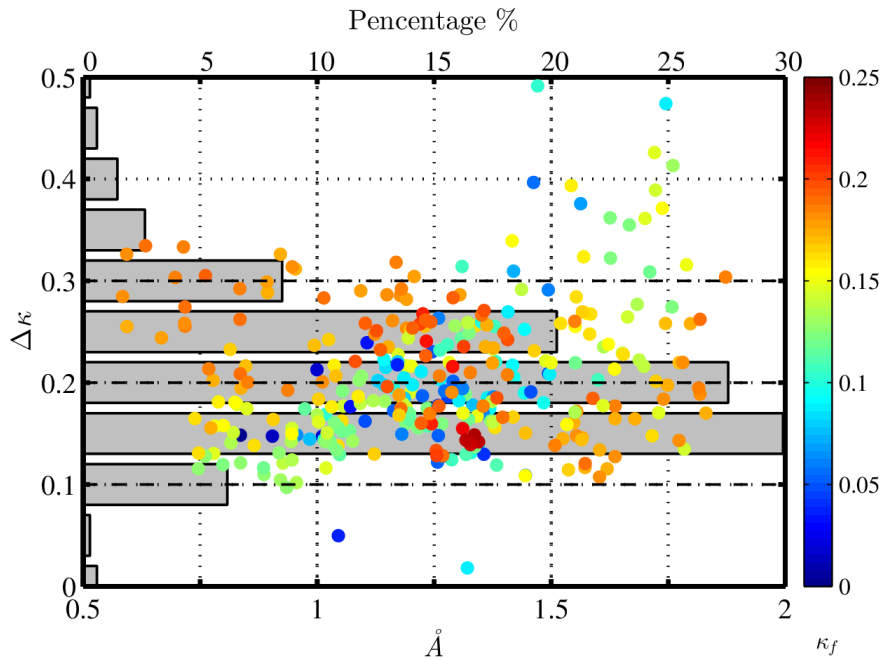


512

513 Figure 4.

514 Overview of measurements in Gucheng in 2016. Upper plot: time series of N_{CCN} at the
 515 supersaturation of 0.07% (red dots), σ_{sp} at the wavelength of 50nm (green dots) and their ratios

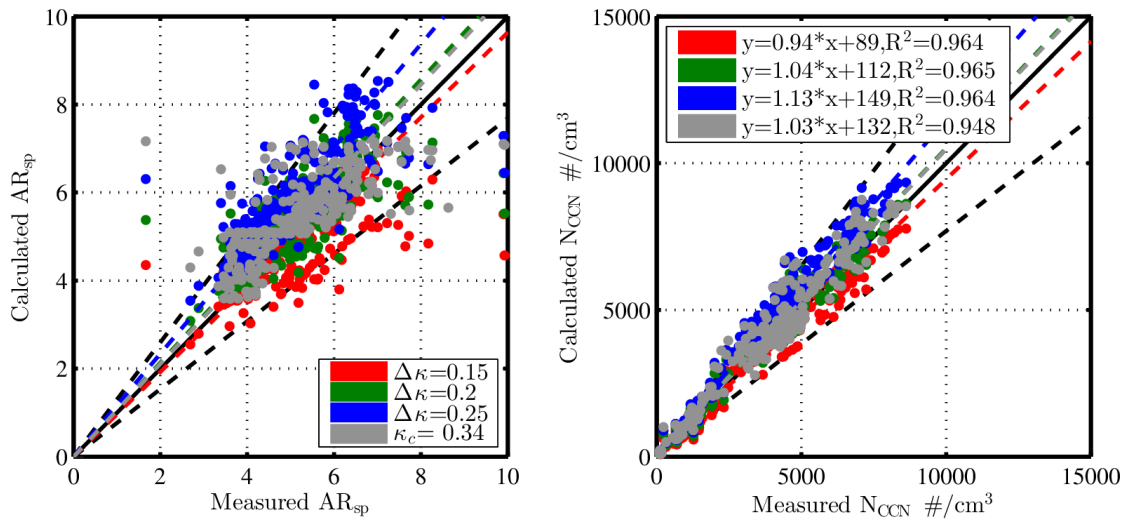
516 (black dots), referred to as AR_{sp} . Lower plot: time series of κ_f (red dots) and \dot{A} (green dots). The
 517 grey bars are periods when the sensitivity of AR_{sp} to κ_c is notable.



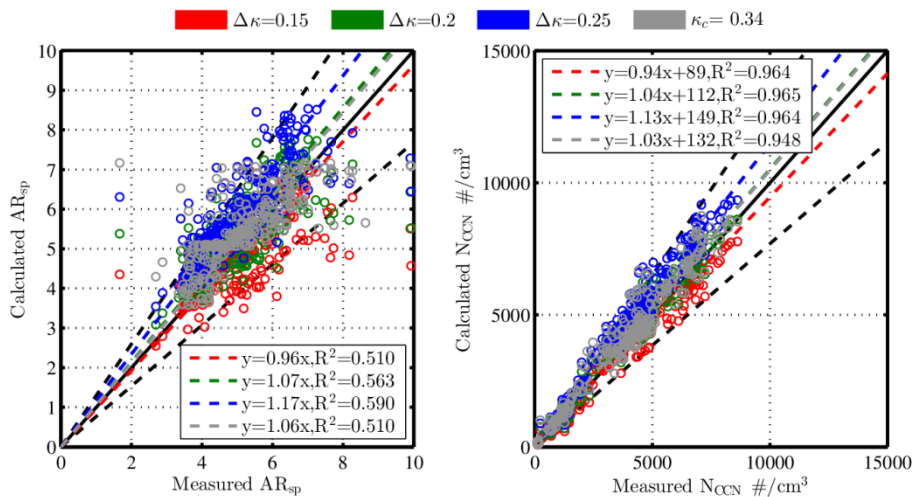
518

519 Figure 5.

520 Differences between κ_c and κ_f , referred to as $\Delta\kappa$, with \dot{A} (positions of dots) and κ_f (colors of
 521 dots). Bars represent percentages of $\Delta\kappa$ within different ranges.



522



523

524 Figure 6.

525 Left plot: comparisons of calculated AR_{sp} and measured AR_{sp} with different conversions of κ_c from

526 κ_f . Right plot: regressions of calculated N_{CCN} and measured N_{CCN} with different conversions of κ_c

527 from κ_f .

528

<u>Campaign</u>	<u>Air mass</u>	<u>Parameter</u>	<u>Caveats</u>	<u>Results</u>	<u>Reference</u>
<u>ICARTT¹ in the north eastern USA and Canada</u>	<u>Polluted air mass</u>	<u>fRH and PNSD</u>	<u>Calculate N_{CCN} with aerosol hygroscopicity constrained by f(RH) and PNSD.</u>	<u>Predict N_{CCN} at SS > 0.3% with a 0.9 R^2.</u>	<u>Ervens et al., 2007</u>
<u>HaChi² on the North China Plain</u>	<u>Aged continental air mass</u>	<u>PNSD and fRH</u>	<u>Similar to Ervens et al., 2007. Calculate N_{CCN} with the hygroscopicity parameter constrained by f(RH) and PNSD.</u>	<u>Slopes around 1 and R^2 around 0.9.</u>	<u>Chen et al., 2014</u>
<u>TARFOX³ Atlantic seaboard and ACE-2⁴</u>	<u>Polluted air mass</u>	<u>Retrieved aerosol volume from remote sensing</u>	<u>Predict N_{CCN} from aerosol volumes with empirical number-to-volume concentration ratio</u>	<u>Overestimate up to 5 times</u>	<u>Gasso and Hegg, 2003</u>

<u>ACE-2 in northeastern Atlantic</u>	<u>Diverse air mass</u>	<u>Backscatter or extinction profile. CCN at the surface.</u>	<u>Retrieve N_{CCN} profile from backscatter (or extinction) vertical profile assuming their ratios are the same to the ratio at surface, which can be calculated by backscatter (or extinction) and N_{CCN} measured at the surface</u>	<u>Predict N_{CCN} on most days for 0.1% SS and on 20%–40% of the days at 1% SS.</u>	<u>Ghan and Collins, 2004</u>
<u>ARM⁵ Climate Research Facility central site at the Southern Great Plains</u>	<u>Continental air mass</u>	<u>Backscatter (or extinction) and RH profile. fRH and CCN at surface</u>	<u>Same as Ghan and Collins, 2004.</u>	<u>Explains CCN variance for 25%–63% of all measurements at high supersaturations</u>	<u>Ghan et al., 2006</u>
<u>TRACE-P⁶ and ACE-Asia⁷</u>	<u>Asian outflow over the western Pacific</u>	<u>Aerosol Index (AI, the product of ambient light extinction and \dot{A})</u>	<u>Predict N_{CCN} based on empirical relationship between AI and N_{CCN}</u>	<u>AI relate well to CCN only with suitably stratified data</u>	<u>Kapustin et al., 2006</u>
<u>Multiple measurements</u>	<u>Diverse air mass</u>	<u>AERONET aerosol optical thickness (AOT)</u>	<u>Predict N_{CCN} based on empirical relationship between AOT and N_{CCN} as a power law</u>	<u>Predict N_{CCN} at SS > 0.3% with a 0.88 R^2, but have a factor-of-four range of N_{CCN} at a given AOT</u>	<u>Andreae, 2009</u>
<u>Four ARM sites</u>	<u>Polluted air mass</u>	<u>SSA, backscatter fraction and σ_{sp}</u>	<u>Estimate N_{CCN} from fitting parameters for the N_{CCN} activity spectra, which can be calculate based on their empirical relationships with aerosol optical properties.</u>	<u>Predict N_{CCN} with slopes around 0.9 and R^2 around 0.6.</u>	<u>Jefferson, 2010</u>
<u>Multiple ARM sites around the world</u>	<u>Diverse air mass</u>	<u>RH, fRH, SSA, AOT and σ_{sp}</u>	<u>Calculate N_{CCN} with σ_{sp} (or AOT) based on their empirical relationship, whose impact RH, fRH and SSA.</u>	<u>Achieve the best results by using σ_{sp} and SSA. Weakly affect on the σ_{sp}-N_{CCN}.</u>	<u>Liu and Li, 2014</u>

relationship by fRH.

Deteriorate

N_{CCN} -AOT

relationship with

increasing RH

Multiple
ARM sites
around the
world

Diverse air
mass not
dominated
by dust

\tilde{A} and
extinction
coefficient

Calculate N_{CCN} with light
extinction based on their
emperical relationship.

Deviate typically
within a factor of 2.0.

Shinozuka
et al.,
2015

529 Tabel 1.

530 Review of studies that have used aerosol optical parameters to infer N_{CCN} .

531 ¹ International Consortium for Atmospheric Research on Transport and Transformation.

532 ² Haze in China.

533 ³ Troposphere Aerosol Radiative Forcing Experiment.

534 ⁴ Second Aerosol Characterization Experiment.

535 ⁵ Atmospheric Radiation Measurement.

536 ⁶ Transport and Chemical Evolution over the Pacific.

537 ⁷ Aerosol Characterization Experiment-Asia.

538